Measurement of an evaporation coefficient in tissue sections as a correction factor for 10B determination

Natalia Espector
Comision Nacional de Energía Atómica (CNEA)
Agustina Mariana Portu (agustina.portu@gmail.com)
Comision Nacional de Energía Atómica (CNEA)
María Sol Espain
Comisión Nacional de Investigaciones Científicas y Técnicas (CONICET), Capital Federal
Gabriela Leyva
Comision Nacional de Energía Atómica (CNEA)
Gisela Saint Martin
Comision Nacional de Energía Atómica (CNEA)

Research Article

Keywords: evaporation determination, tissue sections, BNCT, neutron autoradiography, cryosectioning, water content

Posted Date: April 11th, 2022

DOI: https://doi.org/10.21203/rs.3.rs-1527026/v1

Version of Record: A version of this preprint was published at Histochemistry and Cell Biology on May 1st, 2023. See the published version at https://doi.org/10.1007/s00418-023-02200-w.

Abstract

Boron Neutron Capture Therapy (BNCT) is a cancer treatment option that combines preferential uptake of a boron compound in tumor and irradiation with thermal neutrons. For treatment planning, boron concentration in different tissues must be considered. Neutron Autoradiography using Nuclear Track Detectors (NTD) can be applied to study both boron concentration and microdistribution in tissue samples. Histological sections are obtained from frozen tissue by cryosectioning. When they reach room temperature, they undergo an evaporation process, which leads to an increase of boron concentration in the sample. In order to take this effect into account, certain correction factors (Evaporation Coefficients, CEv) must be applied.

With this aim, a protocol was established in order to register and analyze mass variation of tissue sections, measured with a semimicro scale. Values of ambient temperature, pressure and humidity were simultaneously recorded. Reproducible results of evaporation curves and CEv values were obtained for different tissue samples, which allowed the systematization of the procedure. This study contributes to a more precise determination of boron concentration in tissue samples through the Neutron Autoradiography technique, which is of great relevance to make dosimetric calculations in BNCT.

Introduction

Boron Neutron Capture Therapy (BNCT) is an attractive proposal for cancer treatment. Many advances have been made in basic and clinical research in this field, exploring different targets with a promising outcome (e.g., Chen et al., 2021; Hirose et al., 2021; Kawabata et al., 2021). Unlike conventional treatments, BNCT is a biologically targeted radiation therapy: it ideally allows the irradiation of individual cells or micrometastatic sites with high Linear Energy Transfer (LET) radiation, without affecting the surrounding healthy tissue. It is mainly applied to pathologies that respond poorly to conventional therapies, for different reasons. In many cases it is due to the high heterogeneity of the treated tumors, or to the high sensitivity of the surrounding healthy tissue that acts as a dose limiter, or to the fact that lesions are too small to be correctly detected or are distributed in such a way that radiation damage to healthy tissues cannot be avoided (Coderre et al., 2003).

BNCT is considered as a binary therapy. It requires that a non-toxic compound rich in ^{10}B that preferentially accumulates in tumor cells is infused to the patient. Once the compound is biodistributed in the organism, the region to be treated is irradiated with a thermal or epithermal neutron beam. The charged particles emitted in the boron neutron capture (BNC) reaction deposit a high amount of energy in a range of about a cell diameter. In this way, the tumor cells that have captured ^{10}B atoms are destroyed, while the healthy ones are ideally preserved. For this reason, it is essential to know the distribution and concentration of boron in the different tissue structures when considering a BNCT protocol, especially taking into account that boron uptake may be different depending on the compound to be used in that application.

The Neutron Autoradiography technique using Nuclear Track Detectors (NTD) allows the mapping of heavy particle emitting elements in a sample. Within the framework of BNCT, it means the possibility of knowing the ^{10}B microdistribution in tissue sections. When a boron-loaded tissue section is placed in contact with an NTD and exposed to a thermal neutron flux, the BNC reaction ($10B(n,\alpha)7Li$) occurs. The α and ^{7}Li resulting particles impact the detector generating localized damage in the material, in the surroundings of the ion path (latent tracks). Through a chemical attack process or etching, these latent tracks are revealed and amplified even at light microscopy level, which enables their observation and quantification (e.g. Fleischer et al., 1975). By measuring the number of tracks per unit area (tracks density) observed on the detector and using a previously established calibration curve (Portu et al., 2011), it is possible to estimate the concentration of ^{10}B in the different tissue structures of the original sample. This information is essential in the field of BNCT and allows, for example, the analysis of the uptake pattern of different borated compounds (Portu et al., 2011, 2013).

The histological sections to be studied using this technique are obtained by freezing using a cryostatic microtome (or cryostat). In the transition to room temperature, the tissue undergoes an evaporation process, which generates an increase of ^{10}B atoms concentration in the sample. Furthermore, in the case of soft tissues, evaporation has a direct influence on the tissue section thickness, which at the time of irradiation will be smaller than the nominal thickness set in the cryostat. Thickness of the sample determines the number of particles arriving at the NTD and consequently on the boron quantification (Ceberg et al., 1993). For these reasons a natural amplification of the final number of tracks in the detector occurs.

In order to quantify the boron concentration in the original sample it is necessary to establish correction factors that account for this effect. Since evaporation implies a loss of weight in the sample, and assuming that the quantity of boron atoms does not vary during this process, the concentration can be corrected by an Evaporation Coefficient (CEv), defined as:

$$CEv = \frac{m_s}{m_h}$$

1

Where m_h corresponds to the “wet” section mass, measured immediately after the tissue is sectioned in the cryostat, and m_s is the “dry” section mass, measured when the evaporation process is finished.

The measurement of mass loss is usually carried out through a thermogravimetric analysis (TGA) (Saadatkhah et al., 2020). However, this method requires special equipment, is a destructive technique and takes a long time (2 hours- (Portu et al., 2015)) which reduces the possibility of taking several measurements per day. Hereby, it is necessary to develop a protocol that allows to take measurements using equipment that is widely available, without restrictions on the number of samples to be analyzed.

The problem of tissue evaporation was presented in (Gadan et al., 2012) and the evaporation dynamics was extensively studied in our laboratory (Espector et al., 2018). The proposed correction was applied by Takeno et al. (2021) to consider the effects of water loss on density and elemental composition and was also employed in alpha spectrometry determinations (Bortolussi & Altieri, 2013).

The aim of this work was to explore different aspects involved in the setup of the experimental conditions for the sample mass variation measurement, and to establish a protocol to determine the evaporation coefficients corresponding to different tissues. Systematization of the measurement method also made it possible to create specific software for data recording, visualization, and analysis (EVAP v.2.0). Temperature, pressure and humidity values were registered simultaneously to mass measurements and correction factors associated to environmental conditions were proposed. The protocol was applied to record mass variation due to evaporation in different tissues of interest for autoradiographic analysis, in order to obtain reference values of CEv.

Materials And Methods

A Sartorius Laboratory scale Cubis® line, model MSE125P-000-DU-00 (precision: 10^{-5} g) with USB connection to a notebook was used in this work. Measurements of the mass evolution were taken every 1 s. To characterize the scale drift, 24-hour records of mass values as a function of time were made with different standard weights (Gebrüder Bosch Jungingen / Hohenz) of 20 mg, 50 mg, 100 mg, 200 mg and 500 mg. Simultaneously, temperature, pressure and humidity readings were monitored at intervals of 1 s, using INGKA environmental sensors. Two correction factors were determined to reduce the error associated with the scale drift.

A program designed in Matlab, EVAP v.2.0, was developed to command the whole process of weight determinations over time. The program displays the graph of mass variation as a function of time. It also allows uploading data from temperature, pressure and humidity measurements, and applies the corresponding correction factors. The code selects the first significant mass value and defines it as m_h. As the evaporation takes place, the mass measurements stabilize in about 5 min. Thus, an average of the values recorded between 6 and 12 min was used to obtain the m_s value and calculate the evaporation coefficient.

Tissue samples from normal BDIX rats, nude mice and hamsters were analyzed in this work, being all of them of interest for Neutron Autoradiography analysis in BNCT. Samples coming from a hamster's cheek pouch oral cancer model were also included in the analysis (Kreimann et al., 2001). All the animals were infused with borofenilalanine combined with fructose (BPA-f) according to protocols previously established in each case: for the BDIX rat (Garabalino et al., 2011) and hamster (Kreimann et al., 2001) with a dose of 300 mg / kg and sacrificed 3 h post boron injection and for nude mice (Carpano et al., 2015) of 350 mg / kg and sacrificed 1 h post boron injection. All samples used in this study come from other research groups at BNCT, approved by the institution's Ethics Committee. BDIX rat liver samples were used to design the protocol, due to the uniformity of this tissue at the histological level. In order to

analyze the variation of CEv between species, samples of hamsters and nude mice liver were also included. Furthermore, CEvs were determined in reference tissues (liver, kidney and lung) in BDIX rats.

Sections of the different tissues were obtained by freeze sectioning with a CM 1850 cryostatic microtome from Leica Microsystems. In a previous work it was proved that the difference in thickness sections modifies the evaporation dynamics of the sample but does not affect the CEv final value (Espector et al., 2018). Thus, in order to reproduce the conditions under which an autoradiography is performed, 30 µm and 60 µm nominal thickness sections were obtained and extended on square polycarbonate sheets (2 cm side and 250 µm thick). In previous works, the advantages of using polycarbonate as NTD for the quantification of particles from BNC were established (Saint Martin et al., 2011). The assembly tissue section + polycarbonate was transferred to the scale's weighing chamber in an ice container, to prevent the evaporation process from starting before recording. Registration time was typically 30 min, and once the measurement is finished, EVAP v.2.0 automatically calculates the CEv and generates a document containing all the acquisition information.

The evaporation dynamics obtained through the procedure proposed in this work was compared with the one measured by Thermogravimetry, considered as the reference method. For that purpose, a Shimadzu DTG-50/Simultaneous TG-DTA was set at ambient temperature, without air flux, in order to assure equivalent conditions to those used for the proposed method. The rolled slices were inserted in quartz weighing pans and the mass was registered for 2 h, every 1 s.

In summary, a measurement protocol was established in order to standardize the conditions for all and each sample to be analyzed. Firstly, both registration of the scale and sensors readings are started by the computer. Then the sample is sliced in the cryostat, mounted on a 250 µm thickness polycarbonate sheet, and immediately placed on the scale plate. At the end of the 30-minute acquisition, EVAP v.2.0 calculates the CEv and plots the complete curve of mass as a function of time.

Results And Discussion

The aerostatic driving force is the ascending force of the object that is being weighed (Peña Pérez & Becerra Santiago, 2010). The application of a correction factor (F_{af}) associated with the aerostatic driving force is recommended in the bibliography. The F_{af} (Eq. 2) to be applied to the scale recorded mass value takes into account the air density, which may vary depending on ambient temperature, pressure and humidity:

$$F_{af} = \frac{1 - \frac{\rho_a}{\rho_c}}{1 - \frac{\rho_a}{\rho}}$$

2

where ρ_a is the air density expressed in kg/m^3 (calculated with Eq. 3), ρ_c is the density of the weights used by the manufacturer to calibrate the scale (8000 kg/m^3, corresponding to stainless steel) and ρ is the density of the objects being weighed (2700 kg/m^{3}for aluminum weights).

The air density ρ_a is calculated according to the semi-empirical formula

$$\rho_a = \frac{0.348444p - h(0.00252t - 0.020582)}{273.15 + t}$$

3

where p is air pressure in hPa, h is relative moisture (%), and t is temperature (ºC).

When the F_{af} correction was applied to the standard weights measurements, a minor difference was observed between the measured value and the weight's nominal mass. On the other hand, fluctuations observed during the measurement remained.

These fluctuations turned out to be temperature dependent, moreover each temperature increase detected by the temperature sensor implied a mass decrease, and vice versa. From this observation, an empirical factor related to temperature (T) could be determined:

$$F_e = \left(\frac{T_{inst}}{T_{average}} \right)^{5/m_n}$$

4

where T_{inst} and $T_{average}$ are the instantaneous and mean temperature during measurement, respectively, and m_n is the nominal mass of standard weights expressed in mg.

Thus, the value of corrected mass (m) is given by the simultaneous application of the factors proposed to the scale reading (W), in the form:

$$m = F_{af} * F_e * W$$

5

When applying both the aerostatic and the empirical factors (Eq. 5), records got stable around the nominal value, for the different standard weights. An example of the smoothing effect of these corrections on measurements is presented in Fig. 1.

On the other hand, when analyzing modifications introduced by the correction factors on the CEv calculation, it was observed that only the third decimal place is affected. Therefore, this correction would not be essential in order to obtain a representative CEv. Nevertheless, the corresponding calculation

routine was incorporated in the protocol and in the EVAP v.2.0 code, since it could be useful in future measurements, i.e., in case that extended in time weighing determinations were necessary.

The analysis of measurement uncertainties is essential to estimate the error of the proposed new methodology. Nominal uncertainty of each instrument (Table 1) as well as typical values of every magnitude involved in the process (mass, temperature, pressure and humidity) were considered, and relative errors were calculated. Taking into account Eq. 1, and the correction factors of Equations 3 and 4, the error of the proposed methodology has been estimated as 5%.

Table 1
Instrumental ranges and nominal uncertainties.

Instrument	Range	Nominal uncertainty
Semimicro Scale (Cubis)	0–60/120 g	10^{-5} g / 10^{-4} g
Temperature Sensor (INGKA)	0 - +65°C	0.1°C
Pressure Sensor (INGKA)	300–1100 hPa	0.01 hPa
Humidity Sensor (INGKA)	0–100% RH	10^{-6}% RH

Figure 2 shows a screenshot of the EVAP v.2.0 display. The program was developed to record and analyze mass values as a function of time. It allows the input of the sample identification data, and the duration of the time that the recording will last, which was set as 30 min for all the tissue sections measured in this work. The program plots a graph with the registered values, normalized to the initial mass (m_h). It displays both the starting and the ending times of the record, as well as the calculated CEv value together with a historical value that serves as a reference. Finally, it offers the possibility of loading a file containing a record with the environmental conditions record, that are used to correct the original mass values by applying the previously explained correction factors.

Liver tissue samples were used to establish the new CEv measurement protocol. The data obtained with the proposed methodology was compared with the results of measurements using TGA. Representative curves of both types of measurements are shown in Fig. 3. In order to compare results, the mass values at the *i-th* instant are normalized to the first value (Normalized Mass = m_i / m_h). Since stabilization using TGA is slower and more variable than in the new procedure, subsequent intervals should be considered for the calculation of m_s. The variation in the time elapsed until stabilization is associated with the fact that the geometry of the slice required by the TGA equipment is different from that used in this method. Although the dynamics of the two mass curves as a function of time were different, the final value of the CEv in both cases was equivalent to the historical value of 0.31 ± 0.02 (Portu, Postuma, et al., 2015). The equivalence between CEv values from TGA and the new methodology was also confirmed for lung samples (see Table II).

Mass values as a function of time were recorded using EVAP v.2.0 for BDIX rat liver samples, as it can be seen in Fig. 4. The measurements correspond to tissue sections from the same animal, but under different conditions: (I) different moments along the day, (II) different days, (III) different tissue blocks. The obtained curves were reproducible for the same type of tissue and species, even though the tissue sections had been obtained under different experimental conditions. In every case, it was found that from 0.1 h on, the mass value remains approximately stable. Consequently, the average of mass values recorded in a lapse between 0.1 and 0.2 h (6 to 12 min) was considered to calculate the dry mass m_s.

The CEv values of 38 liver sections coming from different animals were determined, obtaining the distribution shown in Fig. 5. In order to evaluate the normal distribution of this data, a Kolmogorov-Smirnov test was performed, showing that the hypothesis is not rejected at a 5% significance level (with a p-value of 0.20). This indicates consistency in CEv values of tissues from different animals and allows to determine a reference value for liver samples. Therefore, the CEv corresponding to this tissue was established as 0.30 ± 0.02 (mean ± standard deviation), which coincides with the historical value determined by TGA (see Table 2).

The new methodology was then applied to study the evaporation dynamics of liver sections from nude mice and hamsters, besides BDIX rats. As shown in Fig. 6, when analyzing the same type of tissue from different species, no variations are observed in the evaporation dynamics and in the final CEv value (see Table 2).

The protocol developed in this work allowed to determine reference CEv values for some tissues, in order to be used in boron quantification by Neutron Autoradiography. Table 2 shows values obtained for tissues of interest, such as liver, lung and kidney. The measurements were taken from n samples from different animals and each dataset showed a normal distribution, as the one presented in Fig. 5. CEv ranges for liver samples from different species overlap, and the calculated values for rat liver and kidney are equivalent to those reported in Takeno et al., 2021. Furthermore, rat tissue CEvs are consistent with the characteristic water content measured by desiccation in lung, liver and kidney reported in the literature (Reinoso et al., 1997).

Table 2
CEv reference values for different types of tissues, to be applied in boron quantification using Neutron Autoradiography.

Tissue	Species	CEv	Water Content
Liver	NUDE	0.27 ± 0.03 (n = 16)	
Liver	Hamster	0.27 ± 0.03 (n = 17)	
Liver	BDIX	0.30 ± 0.02 (n = 33)	0.705
Kidney	BDIX	0.23 ± 0.02 (n = 19)	0.771
Lung	BDIX	0.20 ± 0.02 (n = 24)	0.790
Metastatic lung	BDIX	0.20 ± 0.03 (n = 16)	
[a] The value coincides with that obtained through TGA (0.32 ± 0.02).			

The value coincides with that obtained through TGA (0.20 ± 0.03).

Reported by Espain et al., 2020.

Reported by Reinoso et al., 1997.

Table 2 also shows the CEv value of samples from the experimental model of disseminated lung metastases of colon carcinoma in BDIX rats (Trivillin et al., 2014). Despite the histological heterogeneities observed in metastatic lung, the CEv values obtained for these cases did not show statistically significant differences. Furthermore, as discussed in Espain et al., 2020, the CEv value of normal lung and lung with metastases are equivalent.

Because of the interest in studying boron microdistribution in different types of tissue coming from a hamster's cheek pouch oral cancer model (Portu, Molinari, et al., 2015), CEv values of samples of tumor, normal pouch tissue and precancerous tissue were measured. The results are presented in Table 3. Although the histology of precancer and tumor tissue may vary between each section, this was not reflected in an increased dispersion. Moreover, normal, precancer and tumor tissue showed similar CEv values.

Table 3
CEv reference values for samples coming from a hamster's cheek pouch oral cancer

Tissue	Species	CEv
Normal Cheek Pouch	Hamster	0.23 ± 0.02 (n = 15)
Precancer	Hamster	0.19 ± 0.01 (n = 12)
Tumor	Hamster	0.18 ± 0.01 (n = 8)

Given that the new methodology allows measurements with equipment commonly found in a laboratory, it proved to be advantageous to obtain reference values. Besides, as it is not a destructive technique, it allows the determination of the CEv corresponding to the same section that will later be used to quantify boron content by Neutron Autoradiography. This advantage is of special interest for the quantification of heterogeneous tissues that could present differences in their evaporation coefficients. Currently, CEv is used not only to take into account the effects of water evaporation on tissue thickness, but also to study the variation in density and elemental composition between dry and wet tissue samples (Takeno et al., 2021). Having an established and reproducible protocol that allows the systematization of the procedure will contribute to a more precise determination of boron concentration in tissue samples through the Neutron Autoradiography technique.

Conclusions

A protocol was established with the aim of studying the mass variation of histological sections due to evaporation, which allows the determination of the CEv with affordable equipment and materials, present in a standard laboratory. A code, EVAP v.2.0, was developed to perform the recording, visualization and analysis of the obtained data. The error of the proposed methodology was estimated at 5%.

The influence of the environmental parameters on the evaporation process was also studied and correction factors were determined to balance ambient fluctuations. On the other hand, it was found that this correction was not necessary for readings carried out under the laboratory environmental conditions, at least for studies performed during 30 min, as those presented in this work.

The designed protocol was applied to determine CEv values for different tissues and species. Reproducible and consistent results were obtained, which allowed to establish a set of reference values.

The proposed methodology for measuring evaporation coefficients is a high-throughput technology that allows many repetitions given its practicability compared to other techniques such as TGA, and it can also be applied to samples of human biopsies. In this case, precise information of the boron uptake pattern in tumor and normal tissue obtained by neutron autoradiography will be of great importance when planning a BNCT treatment.

Declarations

ACKNOWLEDGEMENTS

The authors are grateful with Lic. Marina Carpano and Dr. Alejandra Dagrosa for providing NUDE mice samples, and Dr. Amanda Schwint and collaborators for the hamsters and BDIX rats samples. This work was partially supported by the AGENCIA NACIONAL DE PROMOCIÓN CIENTÍFICA Y TECNOLÓGICA of Argentina through a PICT grant (Nº 2016–0407).

AUTHOR CONTRIBUTION

All authors contributed to the study conception and design. Material preparation, data collection and analysis were performed by N.M.E, A.M.P and M.S.E. G.L. conducted TGA measurements. The first draft of the manuscript was written by G.S.M. and all authors commented on previous versions of the manuscript. All authors read and approved the final manuscript.

References

1. Bortolussi, S., & Altieri, S. (2013). Boron concentration measurement in biological tissues by charged particle spectrometry. Radiation and Environmental Biophysics, *52*(4). https://doi.org/10.1007/s00411-013-0480-y
2. Carpano, M., Perona, M., Rodriguez, C., Nievas, S., Olivera, M., Santa Cruz, G. A., Brandizzi, D., Cabrini, R., Pisarev, M., Juvenal, G. J., & Dagrosa, M. A. (2015). Experimental studies of boronophenylalanine (10BPA) biodistribution for the individual application of boron neutron capture therapy (BNCT) for malignant melanoma treatment. International Journal of Radiation Oncology Biology Physics, *93*(2). https://doi.org/10.1016/j.ijrobp.2015.05.039
3. Ceberg, C. P., Salford, L. G., Brun, A., Hemler, R. J. B., & Persson, B. R. R. (1993). Neutron capture imaging of 10B in tissue specimens. Radiotherapy and Oncology, *26*(2). https://doi.org/10.1016/0167-8140(93)90095-P
4. Chen, Y. W., Lee, Y. Y., Lin, C. F., Pan, P. S., Chen, J. K., Wang, C. W., Hsu, S. M., Kuo, Y. C., Lan, T. L., Hsu, S. P. C., Liang, M. L., Chen, R. H. H., Chang, F. C., Wu, C. C., Lin, S. C., Liang, H. K., Lee, J. C., Chen, S. K., Liu, H. M., … Ono, K. (2021). Salvage boron neutron capture therapy for malignant brain tumor patients in compliance with emergency and compassionate use: Evaluation of 34 cases in Taiwan. Biology, *10*(4). https://doi.org/10.3390/biology10040334
5. Coderre, J. A., Turcotte, J. C., Riley, K. J., Binns, P. J., Harling, O. K., & Kiger, W. S. (2003). Boron Neutron Capture Therapy: Cellular Targeting of High Linear Energy Transfer Radiation. In *Technology in Cancer Research and Treatment* (Vol. 2, Issue 5). https://doi.org/10.1177/153303460300200502
6. Espain, M. S., Dattoli Viegas, A. M., Trivillin, V. A., Saint Martin, G., Thorp, S. I., Curotto, P., Pozzi, E. C. C., González, S. J., & Portu, A. M. (2020). Neutron autoradiography to study the microdistribution of boron in the lung. Applied Radiation and Isotopes, *165*(June), 1–9. https://doi.org/10.1016/j.apradiso.2020.109331
7. Espector, N. M., Portu, A., Santa Cruz, G. A., & Saint Martin, G. (2018). Evaporation process in histological tissue sections for neutron autoradiography. Radiation and Environmental Biophysics, *57*(2). https://doi.org/10.1007/s00411-018-0735-8
8. Fleischer, R. L., Price, P. B., & Walker, R. M. (1975). NUCLEAR TRACKS IN SOLIDS: PRINCIPLES AND APPLICATIONS. *Nucl Tracks in Solids, Princ and Appl*. https://doi.org/10.13182/nt81-a32766
9. Gadan, M. A., Bortolussi, S., Postuma, I., Ballarini, F., Bruschi, P., Protti, N., Santoro, D., Stella, S., Cansolino, L., Clerici, A., Ferrari, C., Zonta, A., Zonta, C., & Altieri, S. (2012). Set-up and calibration of a method to measure 10B concentration in biological samples by neutron autoradiography. *Nuclear*

Instruments and Methods in Physics Research, Section B: Beam Interactions with Materials and Atoms, *274*. https://doi.org/10.1016/j.nimb.2011.11.043

10. Garabalino, M. A., Monti Hughes, A., Molinari, A. J., Heber, E. M., Pozzi, E. C. C., Cardoso, J. E., Colombo, L. L., Nievas, S., Nigg, D. W., Aromando, R. F., Itoiz, M. E., Trivillin, V. A., & Schwint, A. E. (2011). Boron neutron capture therapy (BNCT) for the treatment of liver metastases: Biodistribution studies of boron compounds in an experimental model. Radiation and Environmental Biophysics, *50*(1). https://doi.org/10.1007/s00411-010-0345-6
11. Hirose, K., Konno, A., Hiratsuka, J., Yoshimoto, S., Kato, T., Ono, K., Otsuki, N., Hatazawa, J., Tanaka, H., Takayama, K., Wada, H., Suzuki, M., Sato, M., Yamaguchi, H., Seto, I., Ueki, Y., Iketani, S., Imai, S., Nakamura, T., … Takai, Y. (2021). Boron neutron capture therapy using cyclotron-based epithermal neutron source and borofalan (10B) for recurrent or locally advanced head and neck cancer (JHN002): An open-label phase II trial. *Radiotherapy and Oncology*, *155*. https://doi.org/10.1016/j.radonc.2020.11.001
12. Kawabata, S., Suzuki, M., Hirose, K., Tanaka, H., Kato, T., Goto, H., Narita, Y., & Miyatake, S.-I. (2021). Accelerator-based BNCT for patients with recurrent glioblastoma: a multicenter phase II study. Neuro-Oncology Advances, *3*(1). https://doi.org/10.1093/noajnl/vdab067
13. Kreimann, E. L., Itoiz, M. E., Dagrosa, A., Garavaglia, R., Farías, S., Batistoni, D., & Schwint, A. E. (2001). The hamster cheek pouch as a model of oral cancer for boron neutron capture therapy studies: Selective delivery of boron by boronophenylalanine. Cancer Research, *61*(24).
14. Peña Pérez, L. M., & Becerra Santiago, L. O. (2010, October 27). Impacto de la nueva fórmula de la densidad del aire CIPM-2007. *Simposio de Metrología*.
15. Portu, A., Bernaola, O. A., Nievas, S., Liberman, S., & saint Martin, G. (2011). Measurement of 10B concentration through autoradiography images in polycarbonate nuclear track detectors. *Radiation Measurements*, *46*(10), 1154–1159. https://doi.org/10.1016/j.radmeas.2011.07.034
16. Portu, A., Carpano, M., Dagrosa, A., Cabrini, R. L., & Saint Martin, G. (2013). Qualitative autoradiography with polycarbonate foils enables histological and track analyses on the same section. Biotechnic and Histochemistry, *88*(5). https://doi.org/10.3109/10520295.2012.759624
17. Portu, A., Molinari, A. J., Thorp, S. I., Pozzi, E. C. C., Curotto, P., Schwint, A. E., & Saint Martin, G. (2015). Neutron autoradiography to study boron compound microdistribution in an oral cancer model. International Journal of Radiation Biology, *91*(4), 329–335. https://doi.org/10.3109/09553002.2014.995381
18. Portu, A., Postuma, I., Gadan, M. A., Saint Martin, G., Olivera, M. S., Altieri, S., Protti, N., & Bortolussi, S. (2015). Inter-comparison of boron concentration measurements at INFN-University of Pavia (Italy) and CNEA (Argentina). *Applied Radiation and Isotopes*, *105*. https://doi.org/10.1016/j.apradiso.2015.07.022
19. Reinoso, R. F., Telfer, B. A., & Rowland, M. (1997). Tissue water content in rats measured by desiccation. Journal of Pharmacological and Toxicological Methods, *38*(2). https://doi.org/10.1016/S1056-8719(97)00053-1

20. Saadatkhah, N., Carillo Garcia, A., Ackermann, S., Leclerc, P., Latifi, M., Samih, S., Patience, G. S., & Chaouki, J. (2020). Experimental methods in chemical engineering: Thermogravimetric analysis—TGA. In Canadian Journal of Chemical Engineering (Vol. 98, Issue 1). https://doi.org/10.1002/cjce.23673
21. Saint Martin, G., Portu, A., Santa Cruz, G. A., & Bernaola, O. A. (2011). Stochastic simulation of track density in nuclear track detectors for 10B measurements in autoradiography. Nuclear Instruments and Methods in Physics Research, Section B: Beam Interactions with Materials and Atoms, *269*(23), 2781–2785. https://doi.org/10.1016/j.nimb.2011.08.031
22. Takeno, S., Tanaka, H., Watanabe, T., Mizowaki, T., & Suzuki, M. (2021). Quantitative autoradiography in boron neutron capture therapy considering the particle ranges in the samples. Physica Medica, *82*, 306–320. https://doi.org/10.1016/j.ejmp.2021.02.012
23. Trivillin, V. A., Garabalino, M. A., Colombo, L. L., González, S. J., Farías, R. O., Monti Hughes, A., Pozzi, E. C. C., Bortolussi, S., Altieri, S., Itoiz, M. E., Aromando, R. F., Nigg, D. W., & Schwint, A. E. (2014). Biodistribution of the boron carriers boronophenylalanine (BPA) and/or decahydrodecaborate (GB-10) for Boron Neutron Capture Therapy (BNCT) in an experimental model of lung metastases. Applied Radiation and Isotopes, *88*, 94–98. https://doi.org/10.1016/j.apradiso.2013.11.115

Figures

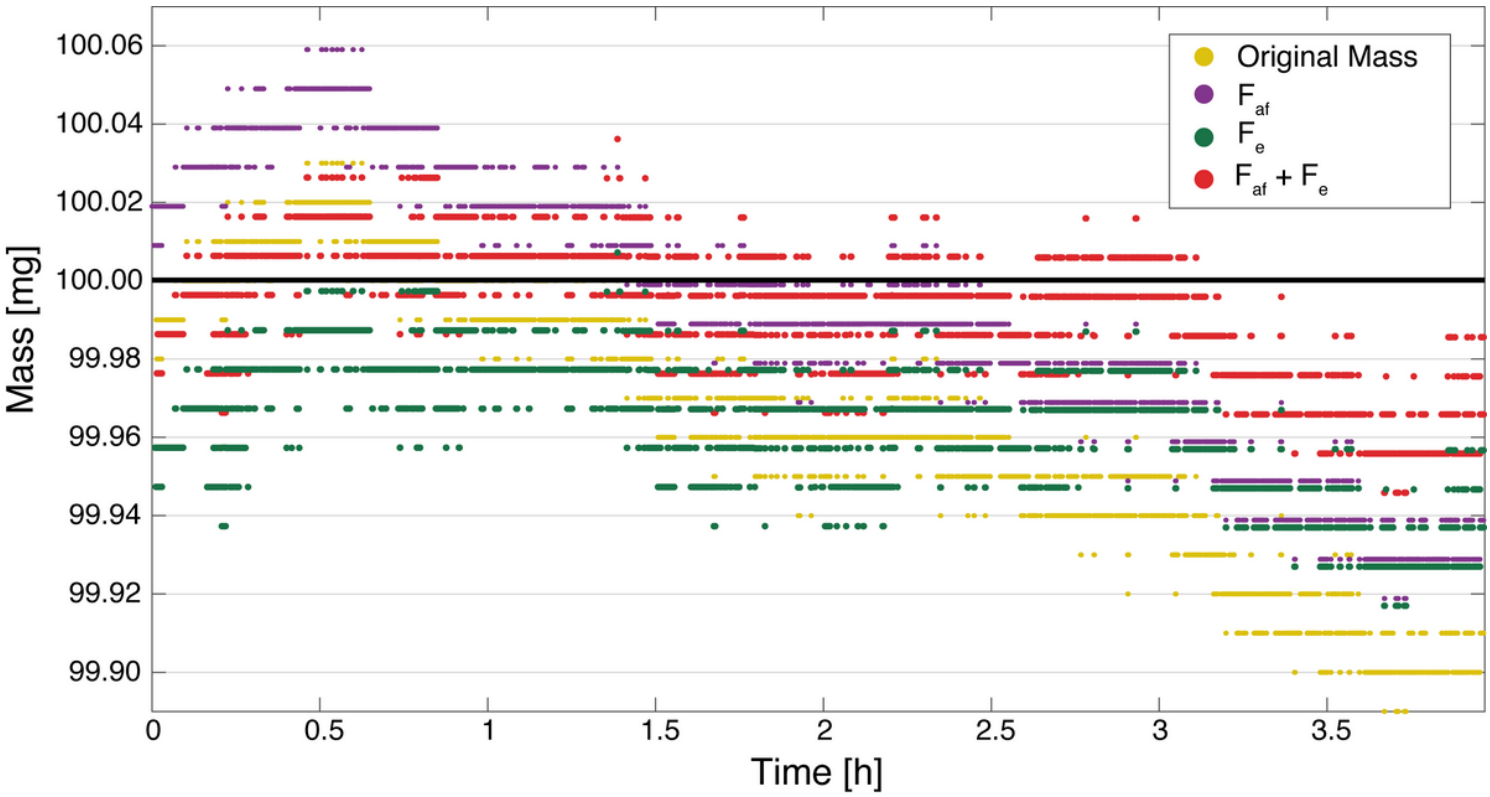

Figure 1

Mass values as a function of time for a 100 mg standard weight without correction (Original Mass), corrected with each proposed factor, and with both factors at the same time. The black line represents the weight nominal mass.

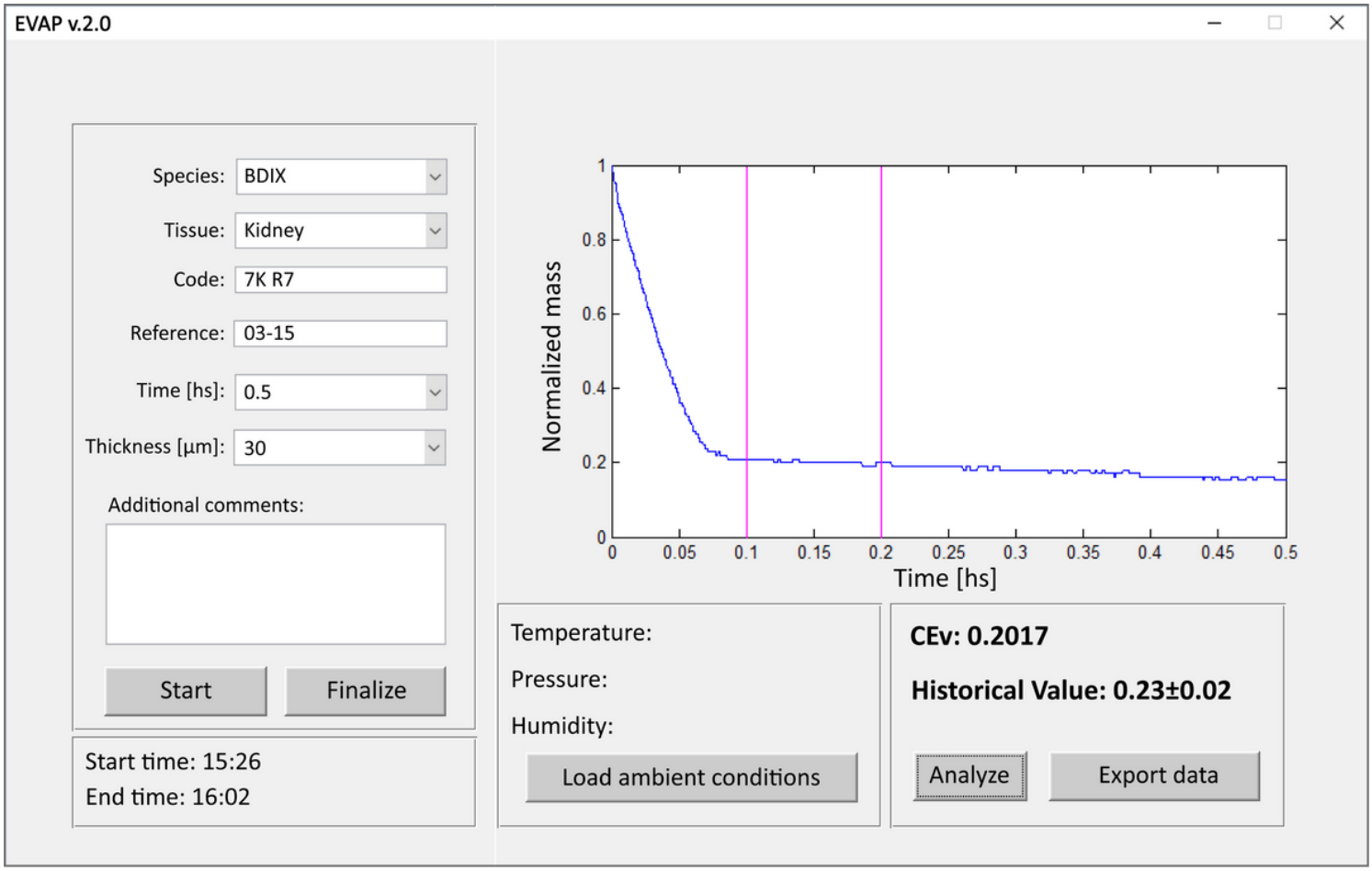

Figure 2

Screen capture of the EVAP v.2.0 display once the measurement is finished.

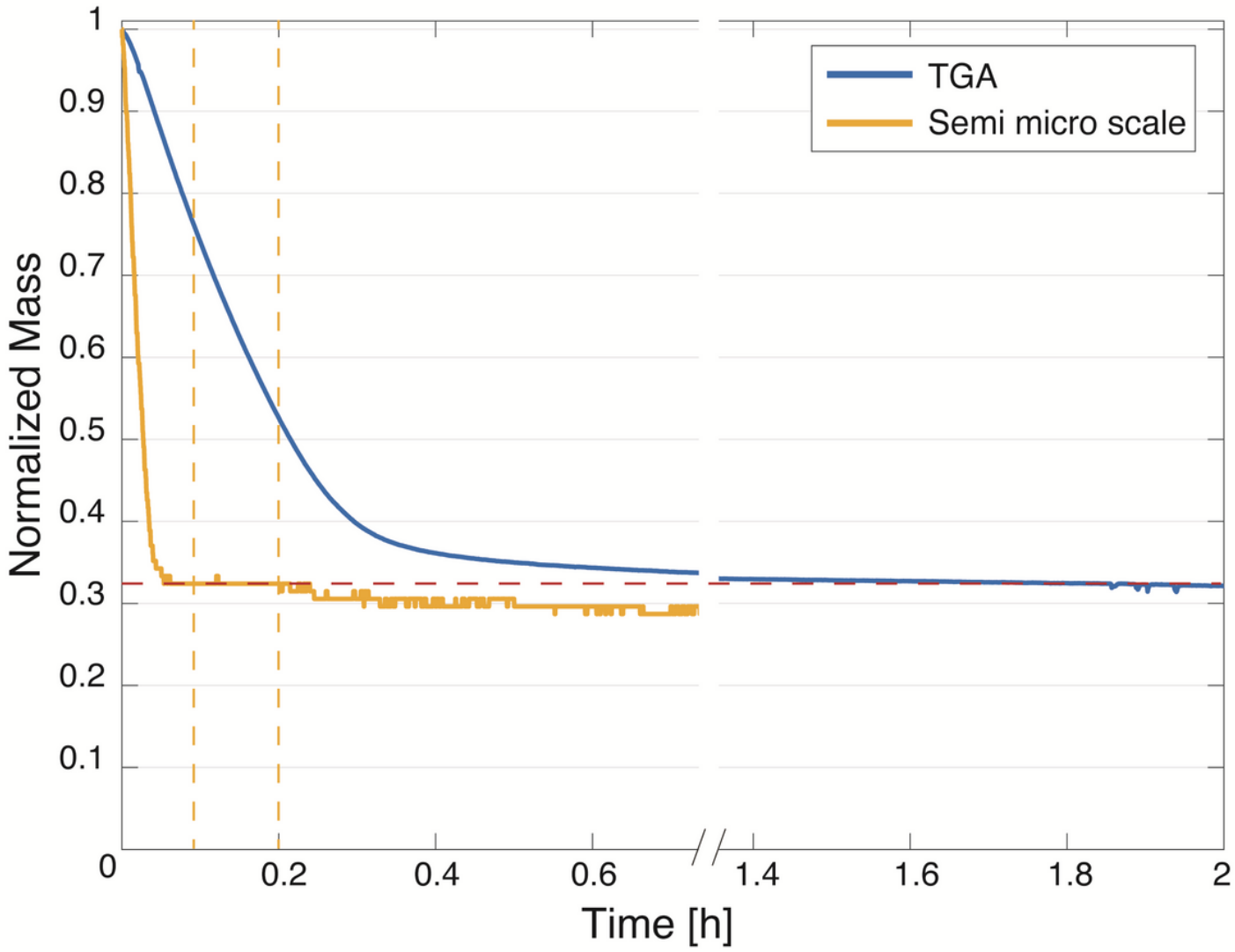

Figure 3

Comparison of BDIX rat liver evaporation dynamics in curves obtained with the presented method (yellow) and with TGA (blue). Yellow dotted line shows the interval that was used to average the values measured with a semimicro scale. The CEv value obtained by both methods (0.32) is shown in red.

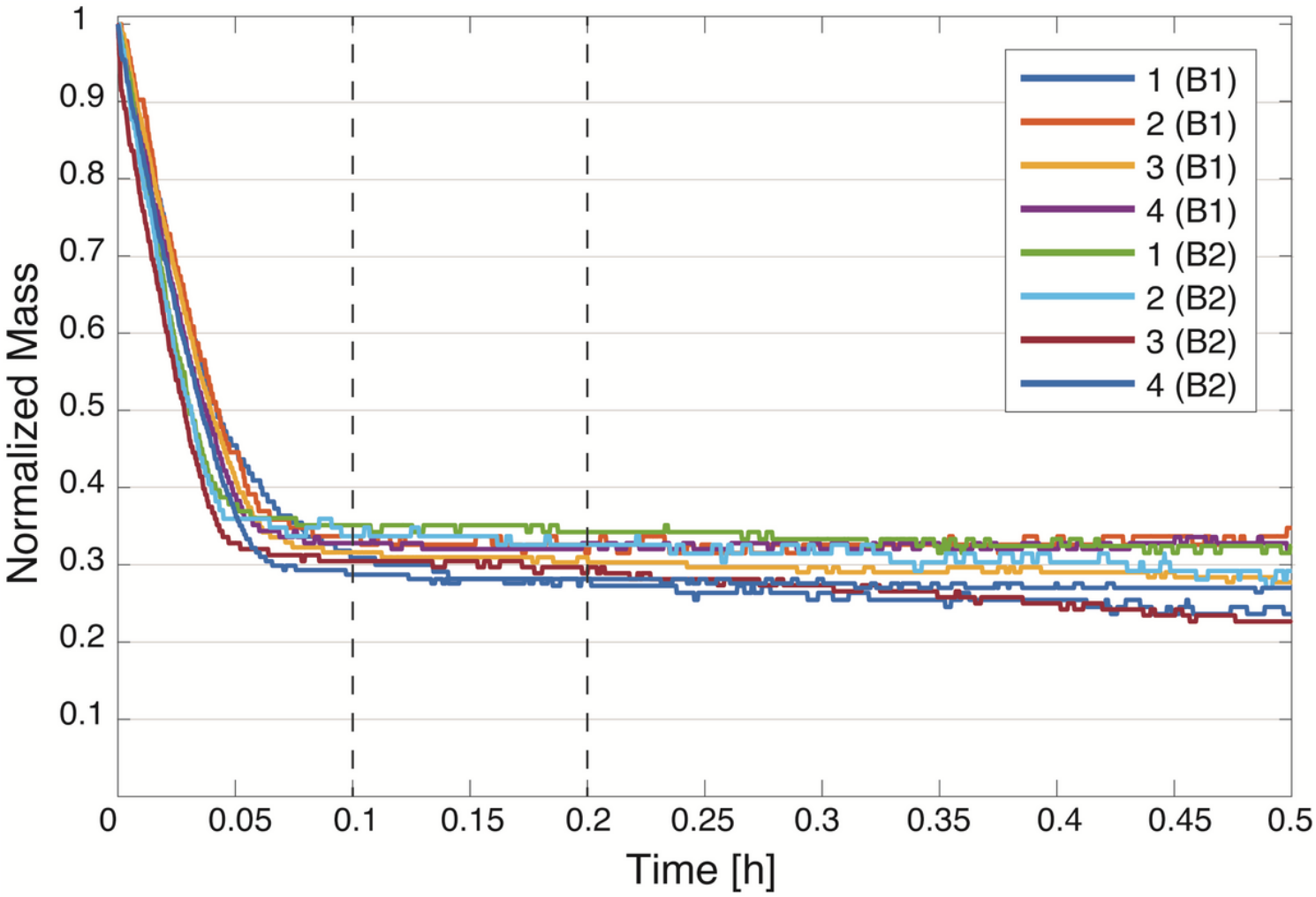

Figure 4

Evaporation dynamics of liver sections from a BDIX rat registered with the new methodology. Tissue sections were obtained under different experimental conditions. B1: Block 1, B2: Block 2. The dotted line shows the averaged interval to obtain the CEv values.

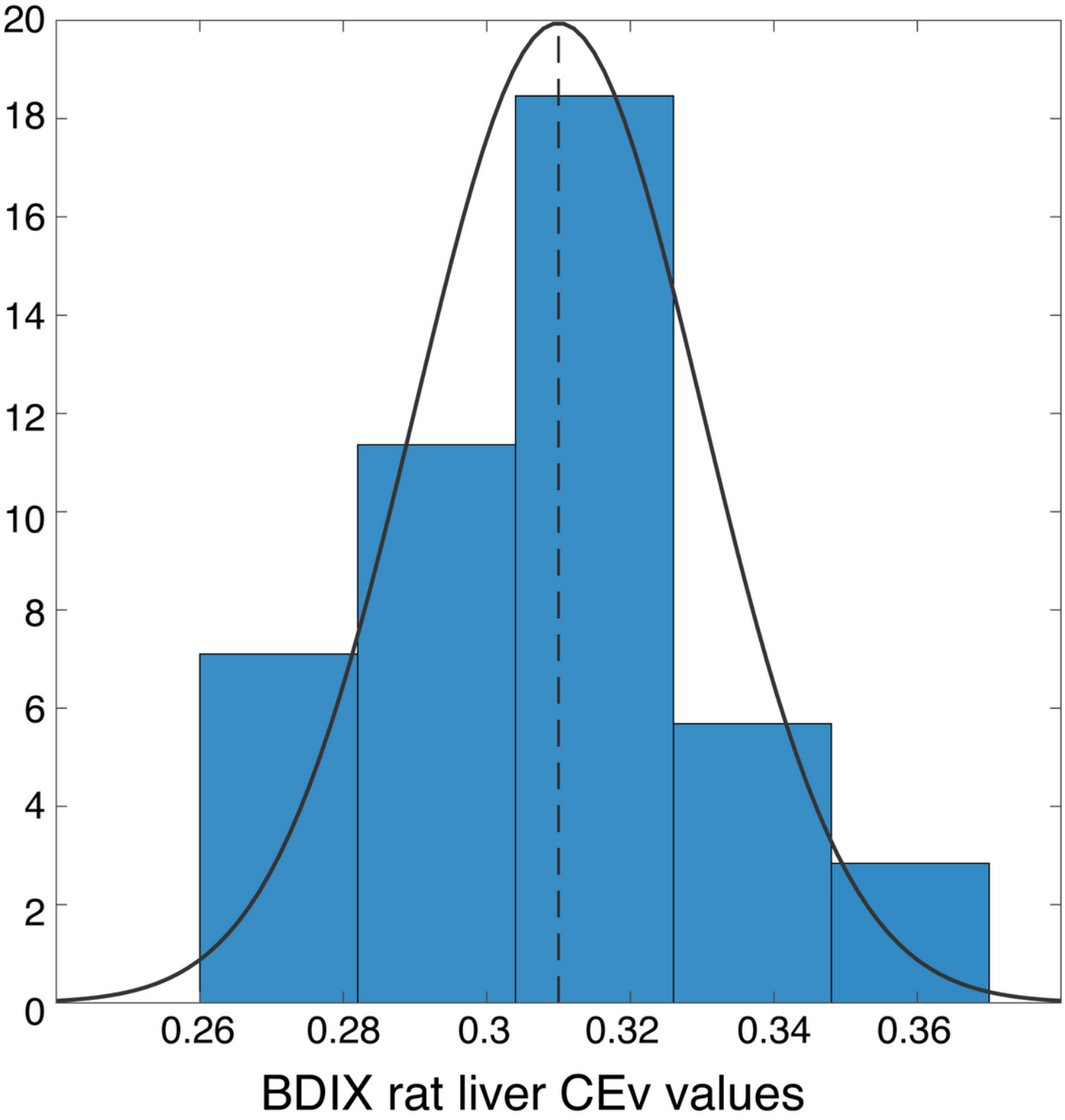

Figure 5

Distribution of CEv values for BDIX rat liver tissue samples. The dotted line shows the mean value of the distribution (0.30). In black the theoretical distribution is presented.

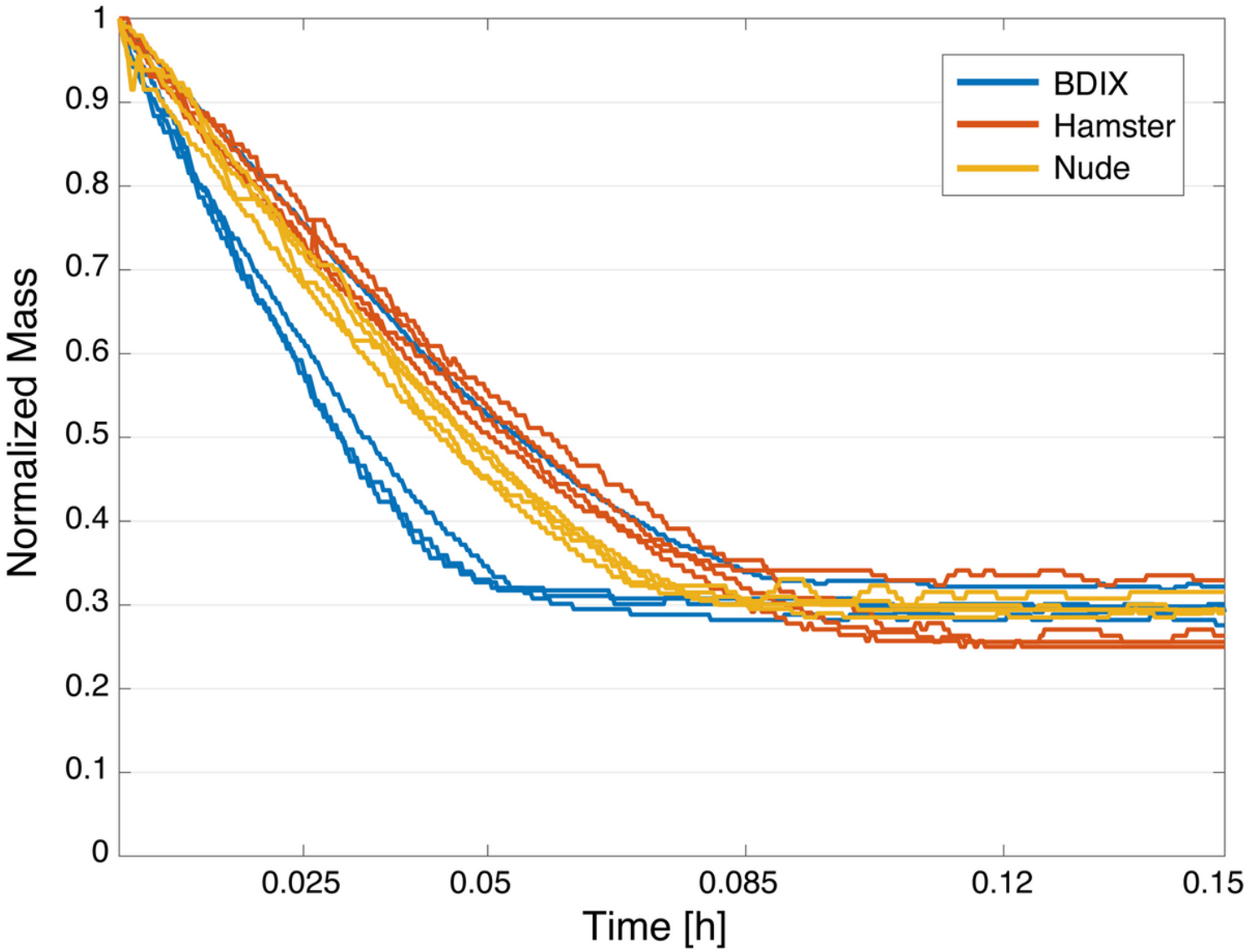

Figure 6

Comparative evaporation curves of liver sections from BDIX rat, nude mice and hamsters.